Precipitation in EB Welded Beryllium Ingot Sheet

Study reveals association of aluminum — rich precipitates with intergranular cracks and reports solute banding in the particular material investigated

BY F. J. FRAIKOR, G. K. HICKEN AND V. K. GROTSKY

ABSTRACT. An investigation was conducted to observe the types, morphology, and behavior of impurity precipitates in beryllium ingot sheet which had been welded by an electron-beam technique. Optical and electron metallography revealed a clear structural transition between the various weld zones.

Transmission electron microscopy of the unaffected zone showed dislocation sub-boundaries 1 to 10 microns in diameter with $AlFeBe_4$ precipitates both in the matrix and

F. J. FRAIKOR is Dean of Engineering, Metro State College, Denver, Colorado; G. K. HICKEN is associated with Sandia Laboratories, Livermore, California; V. K. GROTSY is with the Dow Chemical Company, Rocky Flats Division.

Paper was presented at the 51st Annual AWS Meeting held in Cleveland, Ohio, during April 20-24, 1970.

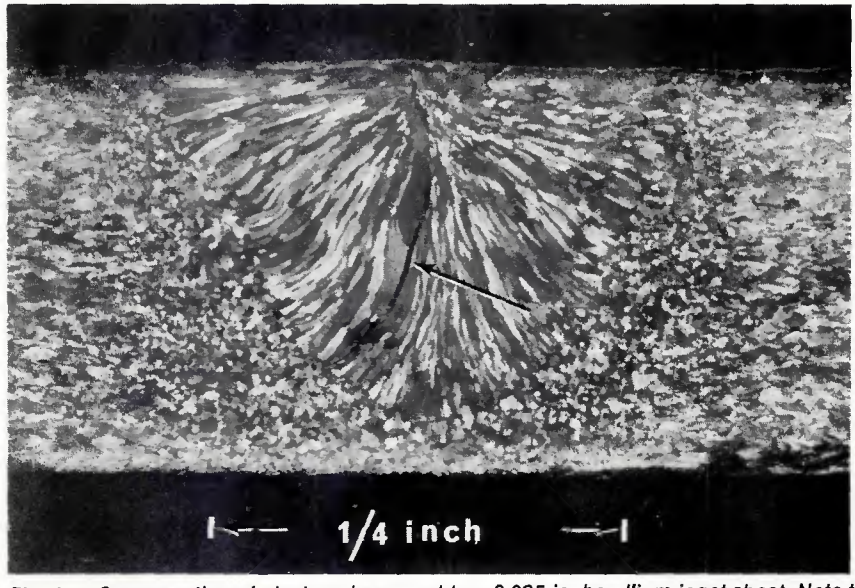

Fig. 1 — Cross section of electron-beam weld on 0.225 in. beryllium ingot sheet. Note the centerline crack (arrow). (Polarized light)

Table 1 — Analysis of 0.225-in. Thick Beryllium Ingot Sheet

Impurity	Original analysis lot 176 CN, weight %	Second analysis lot 176 CN, weight %	Third analysis lot 176 CN, weight %
Aluminum (Al)	0.050	0.080[b]	0.060
Beryllium Oxide (BeO)	0.26 [a]	0.055	—
Carbon (C)	0.065[a]	—	—
Calcium (Ca)	<0.001	0.008	0.003
Cadmium (Cd)	<0.001	0.008	<0.001
Cobalt (Co)	<0.001	0.001	<0.001
Chromium (Cr)	0.015	0.020	0.015
Copper (Cu)	0.020	0.050	0.008
Iron (Fe)	0.185[a]	0.250	0.150
Magnesium (Mg)	0.004	0.007	0.002
Manganese (Mn)	0.018	0.013	0.025
Molybdenum (Mo)	<0.001	<0.001	<0.001
Nitrogen (N)	0.006[a]	—	—
Nickel (Ni)	0.025	0.013	0.025
Lead (Pb)	0.001	0.002	<0.001
Silicon (Si)	0.060	0.070	0.050
Titanium (Ti)	0.020	0.039	0.010
Tungsten (w)	<0.010	<0.010	<0.010
Zinc (Zn)	<0.010	<0.010	<0.010

(a) Chemical analysis; all others by spectroscopic analysis.
(b) Neutron activation analysis.

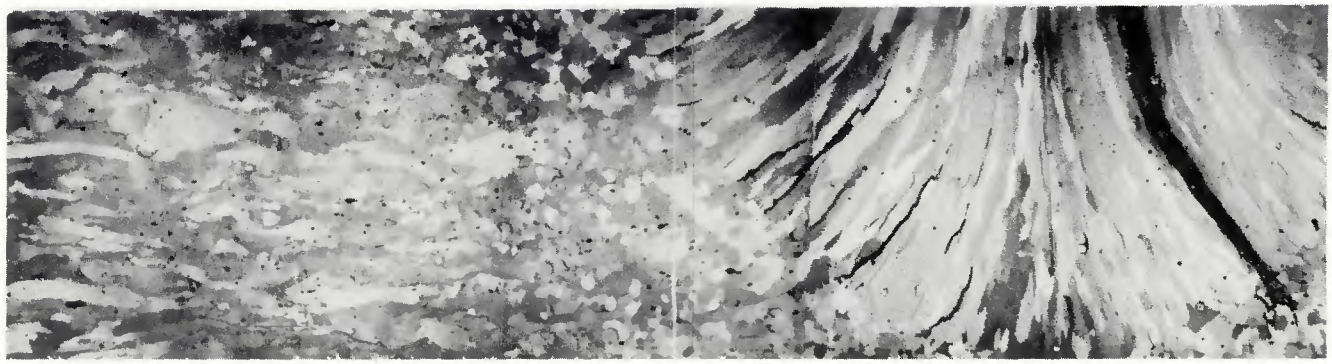

Fig. 2 — Optical photomicrograph showing various weld zones across transverse cross-section of an electron beam welded beryllium sheet specimen. (Polarized light)

Fig. 3 — Optical photomicrograph of the unaffected zone. Note the elongated microstructure of the as-rolled beryllium ingot sheet. (Polarized light, X100, reduced 28%)

Fig. 4 — Optical photomicrograph of the unaffected zone showing the sub boundaries of the as-rolled microstructures. (Bright field, X500, reduced 28%)

sub-boundaries. In areas where the localized weld heating produced temperatures in excess of 900 C followed by moderate cooling, aluminum-rich grain boundary precipitates were found. Electron-microprobe scanning of weld cracks revealed that these aluminum-rich precipitates introduce *hot-short* liquid areas which, combined with thermal stresses, produce intergranular cracks.

Transmission photomicrographs further showed that the *solidification bands* consisted of rows of both irregular shaped $AlFeBe_4$ precipitates and platelets of $FeBe_{11}$ interconnected by dislocation sub-boundaries. It is postulated that these solidification bands are produced by solidification fluctuations with resultant microsegregation of iron and aluminum.

Introduction

Considerable attention has been focused on the joining of beryllium, since this material has found increasing applications, particularly in aerospace and nuclear fields. A review of the techniques, problems, and successes associated with the joining of beryllium can be found in reports and articles such as those by Hicken[1,2] and Hauser.[3,4]

Hauser and coworkers[3], for example, have demonstrated the role of varying beryllium oxide content on the formation of sound electron beam welds. They found that reducing the beryllium oxide in the starting material consistently reduced the amount of undercutting, porosity, and surface roughness of the welds. Furthermore, in a similar investigation, Hauser and Monroe[4] found indications of extensive precipitation in some of the weld areas and felt that intergranular cracking could be related to unidentified grain-boundary precipitation.

At the same time, other studies[5-15] have demonstrated the role of various impurities, particularly iron and aluminum in precipitation reactions in beryllium. The predominant precipitates in the microstructure of commercial purity beryllium are of the ternary type, $AlMBe_4$, and the binary type, MBe_{11}. The *M* in the formula is one of the transition elements: iron (Fe), chromium (Cr), nickel (Ni), or manganese (Mn). The precipitation

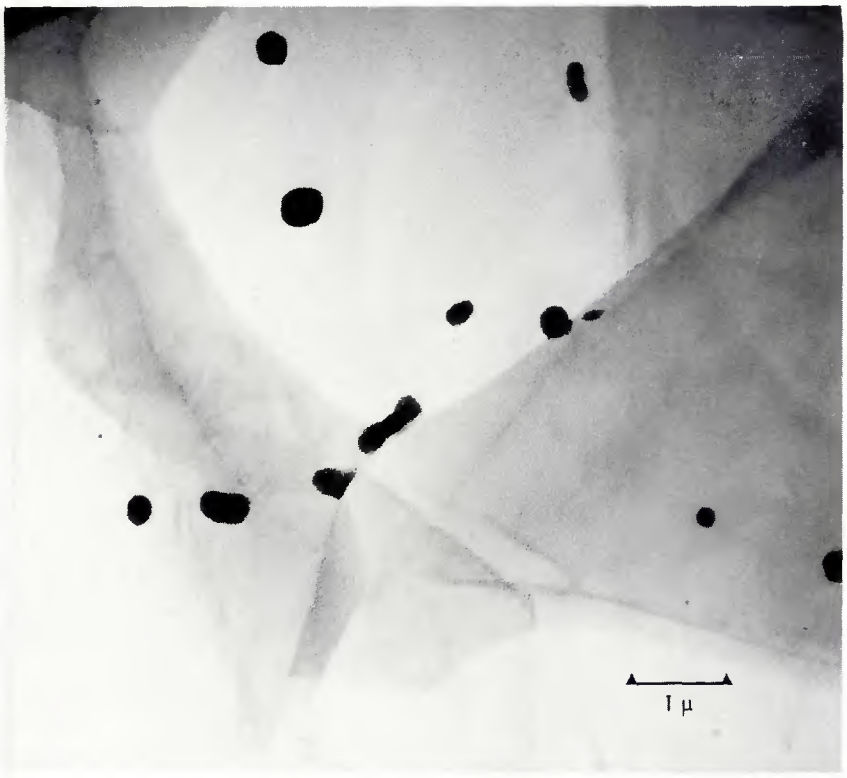

Fig. 5 — Transmission electron photomicrograph of the unaffected zone of the beryllium ingot sheet. Note the dislocation sub-boundaries and the globular shaped $AlFeBe_4$ precipitates

characteristics are dependent on the impurity content and the heat treatment history of each particular beryllium lot. In the case of beryllium ingot sheet currently produced at Rocky Flats, the predominant metallic impurity element is Fe so that $AlFeBe_4$ and $FeBe_{11}$ are the resultant types of precipitates generally observed in the microstructure. Hence, it appeared feasible to make a comparison of the precipitation characteristics of Rocky Flats beryllium ingot sheet after various heat treatments[11-15] with those observed in the various zones of an electron beam welded sample of the same origin. Furthermore, the oxide content of this ingot sheet is extremely low (0.055 weight % by neutron activation analysis). Thus, the problems associated with beryllium oxide in the weld metal as noted by Hauser would be minimized.

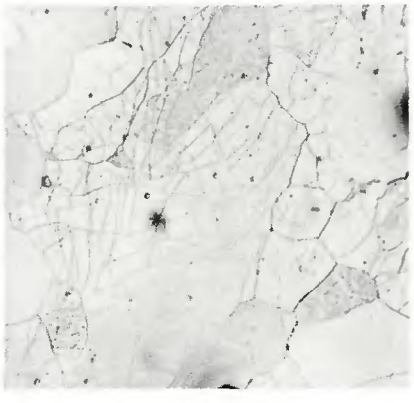

Fig. 6 — Partly recrystallized zone. Note the equiaxed recrystallized grains among the substructure of the as-rolled beryllium ingot sheet. (Bright field, X400, reduced 43%)

The objective of the current investigation was to observe the types, morphology, and behavior of impurity precipitates in the microstructure of electron beam welded beryllium specimens. It should be emphasized that no attempt was made to optimize the welding parameters and the resultant welds. Instead, a variety of welds were produced including samples with wide fusion and heat-affected zones similar to those produced in gas tungsten-arc welds.

Experimental Procedure

The material utilized in this investigation was 0.225-in. thick Be ingot sheet, rolled from vacuum-cast ingots at the Rocky Flats Division of The Dow Chemical Company. The chemical analysis of the Be sheet is shown in Table I. The sheet was in the as-rolled condition with no post-rolling heat treatments. However, the surface had been chemically etched to remove surface oxides and rolling lubricants.

A high voltage, 6-kilowatt (kW), electron beam welding machine was used to make bead on plate welds on the Be sheet. Although a variety of weld sizes was produced, the specimens with exaggerated weld zones were particularly useful for subsequent examination by transmission electron microscopy. The welding parameters used in this instance were an accelerating voltage of 130 kilovolts (kV) with a beam current of 40 milliamperes (mA) and a part velocity of 20 ipm in a vacuum of 5×10^{-5} torr. The beam-spot size was 0.220 in. in diam and was focused at approximately ⅛ in. below the surface. These welding conditions produced intense heating over a wide area with such shallow penetration that the depth-to-width ratio was only 1 to 1. A cross-section of a weld with exaggerated weld zones and cracks is shown in the optical photomicrograph of Fig. 1. Other welds with depth-to-width ratios greater than 3 to 1 apparently produced crack free welds, but the heat-affected zone was too narrow for effective metallographic examination. Little porosity was noted in any of the specimens.

The metallographic techniques employed for optical examination of the weld microstructures included illumination by both bright field and polarized light. Specimens to be examined by polarized light were sectioned by a diamond saw or chemical saw, mounted and rough-ground through 600-grit silicon carbide paper using water as a lubricant. Polishing was continued down through 1-micron diamond paste on a Nylon cloth with deodorized kerosene lubricant and subsequently placed on a Syntron for final polishing overnight with 0.03-micron alumina on a Gamel cloth. The lubricant for final polishing was a slurry of 10 milliliters (ml) of chromic acid in 600 ml of water. The final step was not used for specimens which were to be subjected to electron microprobe analysis because of the possibility of alumina contamination in voids, cracks, etc.

Although polarized light illuminations successfully revealed the transition between the various weld zones (Fig. 2), bright field illumination of electrolytically polished and etched specimens was necessary to clearly resolve the substructure in some portions of the weld. Details of the technique can be found in Reference 14.

The most difficult portion of the metallographic techniques was the preparation of thin films from the weld for transmission electron microscopy, particularly since various zones of the weld tend to thin electrolytically at

varying rates. To some extent, the problem was solved by masking selected areas on the face of the specimen with lacquer, thus thinning only the desired portion of the weld sample. The electrolytic thinning was accomplished in a Glenn Dual Jet thinning unit using an electrolyte of 400-ml ethylene glycol, 40 ml of nitric acid (HNO_3), 8 ml of sulfuric acid (H_2SO_4), and 8 ml of hydrochloric acid (HCl), with a current of approximately 900 mA at 36 V. The electrolyte was kept at a temperature of 10 to 15 C by a surrounding ice water bath.

The thin foils were then immersed in hot distilled water, rinsed in methyl alcohol, and then mounted between 75 mesh copper grids and examined at 100 kV in a Philips EM-200 electron microscope.

Results and Discussion

Optical and electron metallography revealed a clear structural transition in some specimens between the various weld zones as illustrated in the low magnification photograph of Fig. 2. Beginning with the unaffected zone at the edge of the Be sheet, the specimen exhibited the expected correlation between the temperature gradient and the microstructure.

Unaffected Zone

The as-rolled condition of the unaffected portions of the weld samples consisted of a *warm-worked* substructure of dislocation cell walls and sub-boundaries (Figs. 3, 4, and 5). Such a microstructure is the result of rolling the beryllium sheet slightly below the recrystallization temperature so that little or no recrystallization occurs during and after the final rolling pass. The subgrains are 1 to 10 microns in diam, although the size varies depending on the thermal and rolling history of each particular billet.

In addition to the cellular structure, globular-shaped precipitates 500 to 5000 angstroms in diam are found scattered intermittently throughout the microstructure of the unaffected zone (Fig. 5). These particles were identified by electron diffraction techniques[12] as mainly of the ternary type termed $AlFeBe_4$ by Carrabine[9] or Be_5 (Fe, Al) by Rooksby[8] with a face-centered cubic lattice parameter of approximately 6.05 angstroms. In addition, some platelets of the binary precipitate, $FeBe_{11}$ were also observed.

The microstructure of the unaffected zone of the beryllium ingot sheet then can be characterized as consisting of dislocation sub-boundaries with incoherent, globular $AlFeBe_4$ precipitates scattered throughout this warm-worked structure. It should be pointed out that Rocky Flats beryllium ingot sheet is generally supplied in the annealed condition; that is, the sheet has undergone a 15 to 20 hr anneal at around 780 C. In this case, complete recrystallization occurs to a grain size of 40 to 60 microns and some precipitates coalesce to larger sizes.[12] Lesser annealing times or lower temperatures produce recovered and partly recrystallized microstructures. Such heat treatment approximately corresponds to the first heat-affected zone of the electron beam weld.

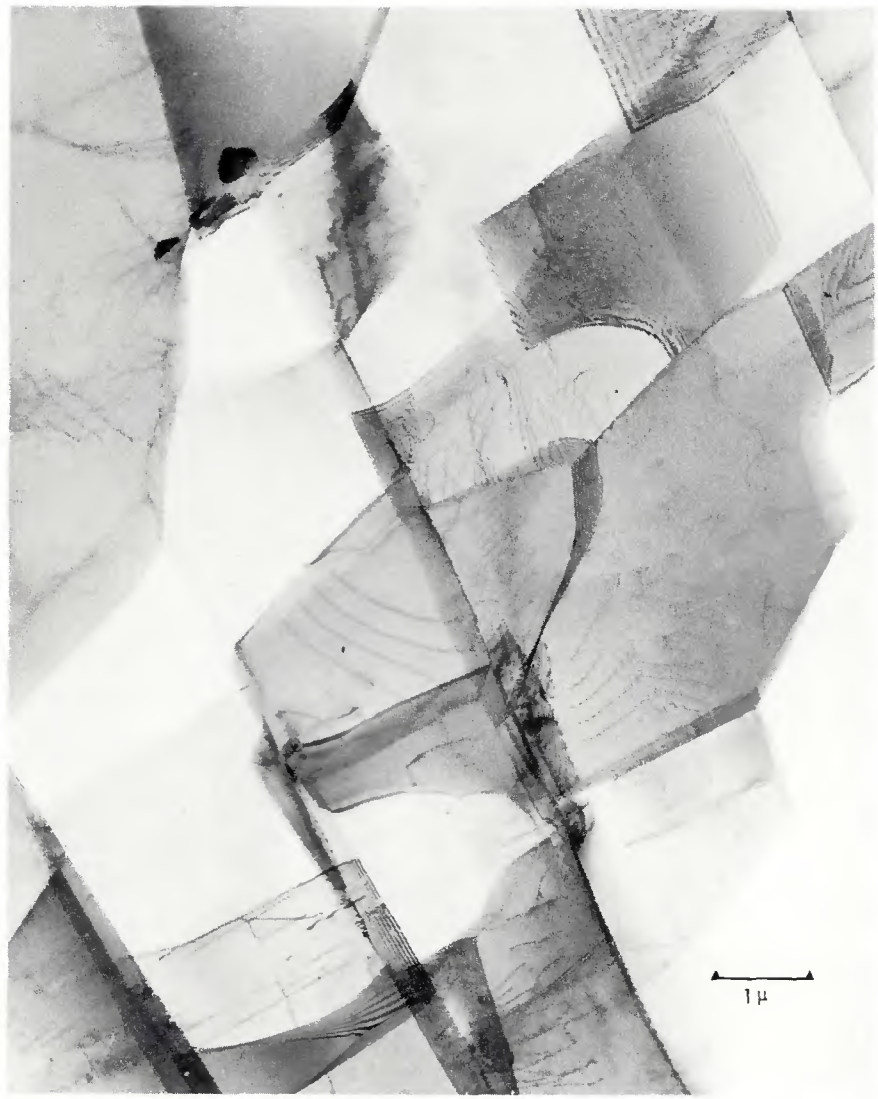

Fig. 7 — Shows dislocation arrays and well defined sub-boundaries as a result of polygonization at the outer edge of the heat-affected zone

Partly Recrystallized Zone

Figures 6 and 7 show the microstructure of the partly recrystallized area of the weld specimen. Figure 6 is an optical photomicrograph taken under bright field illumination and the etch clearly shows some new equiaxed grains among the as-rolled substructure. The transmission electron photomicrograph in Fig. 7 further reveals that recovery by the process of polygonization has taken place in the remaining as-rolled substructure. That is, sufficient thermal energy was provided at this weld perimeter to allow the dislocations to migrate into narrower cell walls and to assume more metastable equilibrium con-

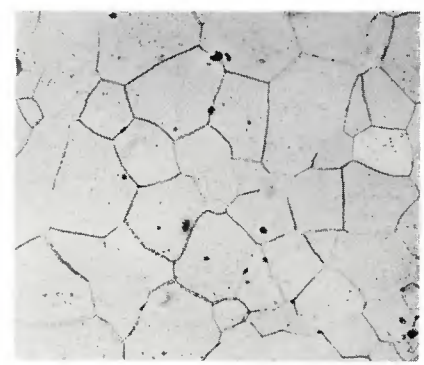

Fig. 8 — Shows fully recrystallized portion of the heat-effected zone. Grain size is 40 to 75 microns. (Bright field, X300, reduced 43%)

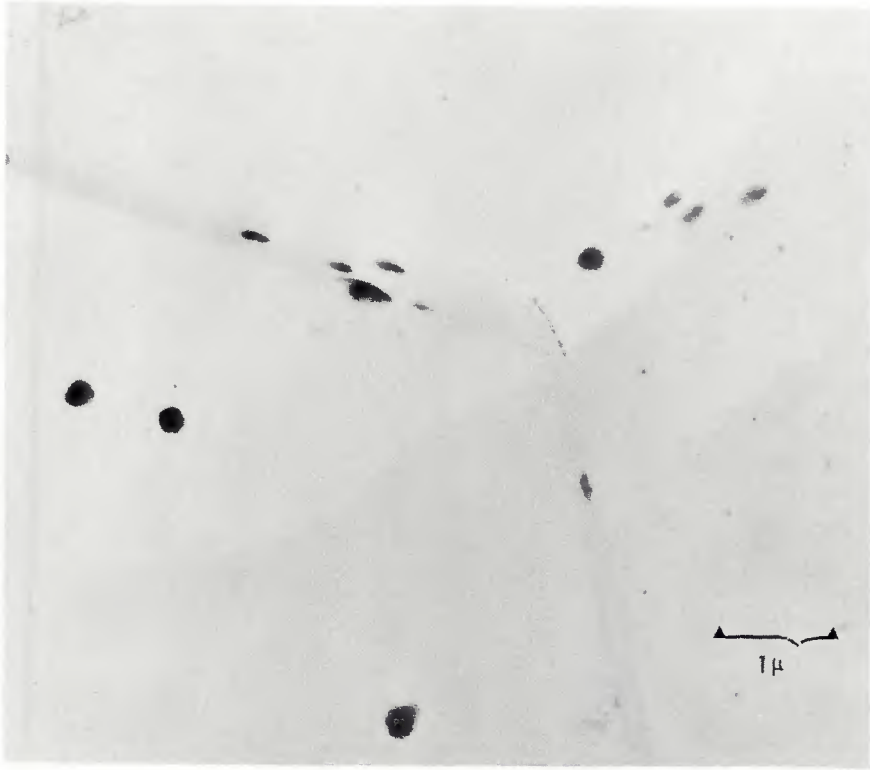

Fig. 9 — Aluminum-rich precipitates in the matrix and grain bounderies of the recrystallized zone

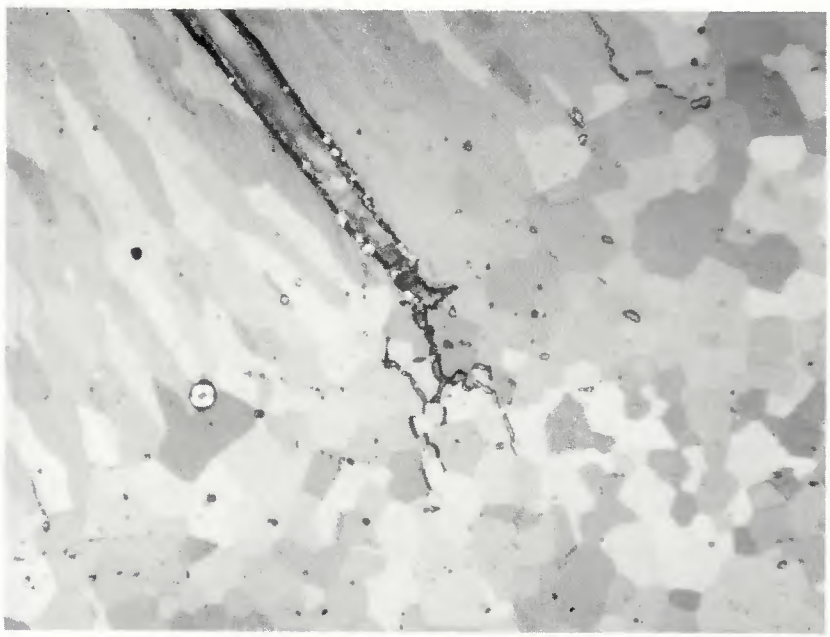

Fig. 10 — Intergranular cracks in the heat-affected zone. Note that some of the cracks continued to propagate into the fusion zone. (Polarized light, X75)

figurations in the form of regular arrays. Precipitation in this area was not greatly affected by the electron beam heating, although the existing precipitates do tend to inhibit boundary migration in some instances. However, closer to the weld where temperatures in excess of 900 C were achieved, complete recrystallization and grain growth were accompanied by significant changes in the precipitates.

Recrystallized Zone

Complete recrystallization in the heat-affected zone resulted in a grain size of approximately 40 to 75 microns in size (Fig. 8, optical photomicrograph). More significant was the appearance of aluminum-rich precipitates, particularly in the grain boundaries as shown in the transmission electron photomicrograph in Fig. 9. In most instances these precipitates are much too small (less than 0.1 micron) to be seen by optical microscopy. However, at the fusion zone and heat-affected zone interface, precipitation was more extensive and accompanied by intergranular cracking. Often these intergranular cracks propagated along the epitaxial columnar grains at the fusion zone interface. These cracks continued along the columnar grain boundaries in the fusion zone and finally terminated at the centerline of the weld (Fig. 10, optical photomicrograph).

In an effort to determine a possible relationship between the intergranular cracks and precipitation in the beryllium, extensive optical and electron metallography was done on the fusion zone — heat-affected zone interface. In addition, electron microprobe analysis was directed along the beginnings of the intergranular cracks.

The results reveal an association of aluminum-rich areas with the intergranular cracks. For example, Fig. 11 (a) shows three small cracks along the grain boundaries in the fully recrystallized portion of the heat-affected zone. These particular cracks were chosen for examination because they did not extend into the fusion zone and, therefore, clearly originated in the heat-affected zone of the electron beam weld. A raster scan of aluminum-Kα radiation was then performed on this area. Although the data were qualitative, Fig. 11 (b) shows that aluminum is present along the crack areas.

Furthermore, transmission electron microscopy in the vicinity of microcracks revealed extensive grain boundary precipitation as illustrated in Fig. 12. This observation confirms the association of intergranular cracks in beryllium welds with grain boundary segregation noted by Hauser and Monroe[4] by replica techniques. Diffraction patterns from these large precipitates were generally complex, but in some instances the particles could be analyzed as of the $AlMBe_4$ type. On the basis of previous studies[11,12,13] of quenching Rocky Flats Be ingot sheet from above 900 C, aluminum-rich, grain boundary precipitates can be expected with moderately rapid cooling rates. Whereas, slower cooling rates permit transition element diffu-

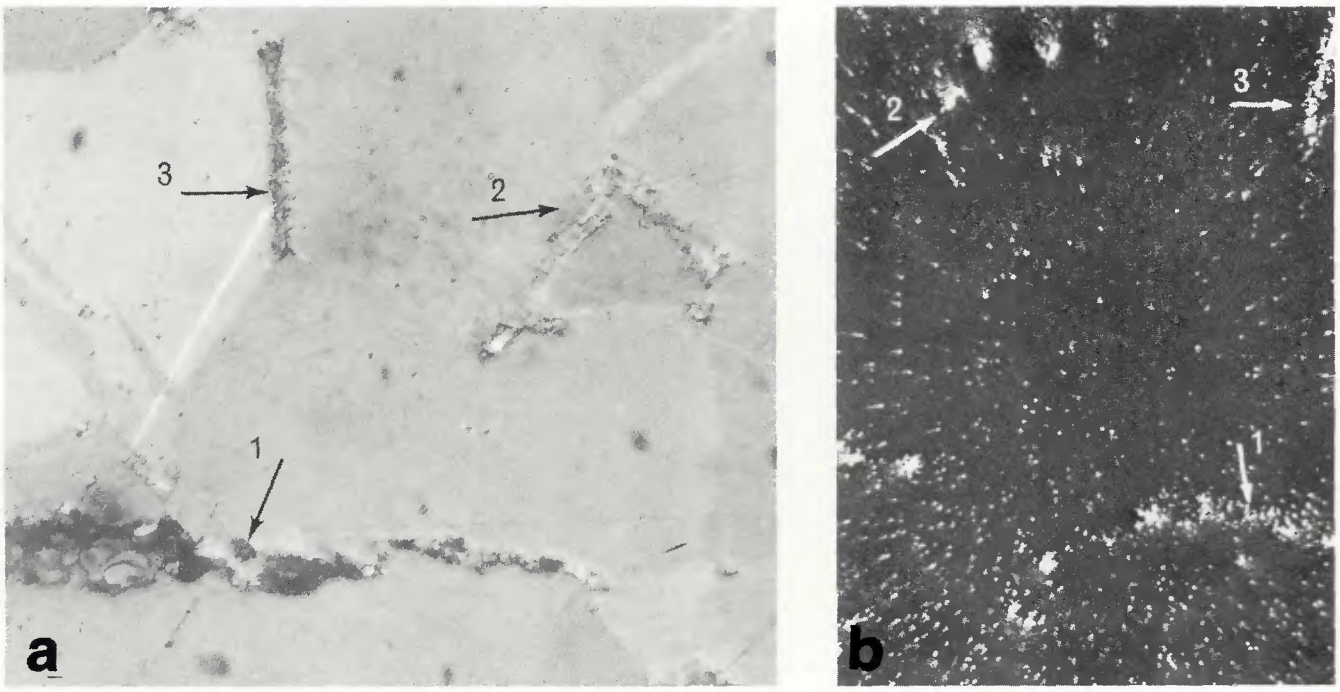

Fig. 11 — Optical photomicrograph of recrystallized area (a) showing three intergranular cracks (marked 1, 2 and 3); (b) Raster scan (aluminum-Kα radiation) of the intergranular crack area

sion to form $AlMBe_4$ at the grain boundaries in such material.

Nonetheless, it is reasonable to assume that these large aluminum-rich precipitates in the grain boundaries of the recrystallized grains introduce *hot-short* liquid areas which, combined with thermal welding stresses, produce the observed intergranular cracking. Although cracks generally originate in the heat-affected zone, the epitaxial relationship of the adjacent fusion zone grains permits easy propagation of the cracks across the fusion zone interface. Again it should be emphasized that these cracks were found only in the extremely wide and shallow weld specimens, and can generally be avoided with normal electron beam welding conditions.

Fusion Zone

An interesting feature of the fusion zone of the electron beam welds in the ingot sheet was the appearance, after proper electro-polishing, of *transverse solute bands*. These were more pronounced near the edge of the fusion zone and were approximately normal to the direction of solidification (Fig. 13, optical photomicrograph). D'Annessa[16] has attributed this phenomenon to cyclic variations in growth rate, resulting from thermal fluctuations in the weld pool. Therefore, it was particularly interesting to directly observe the fusion zone microstructure by transmission electron microscopy in an effort to identify the origin of these

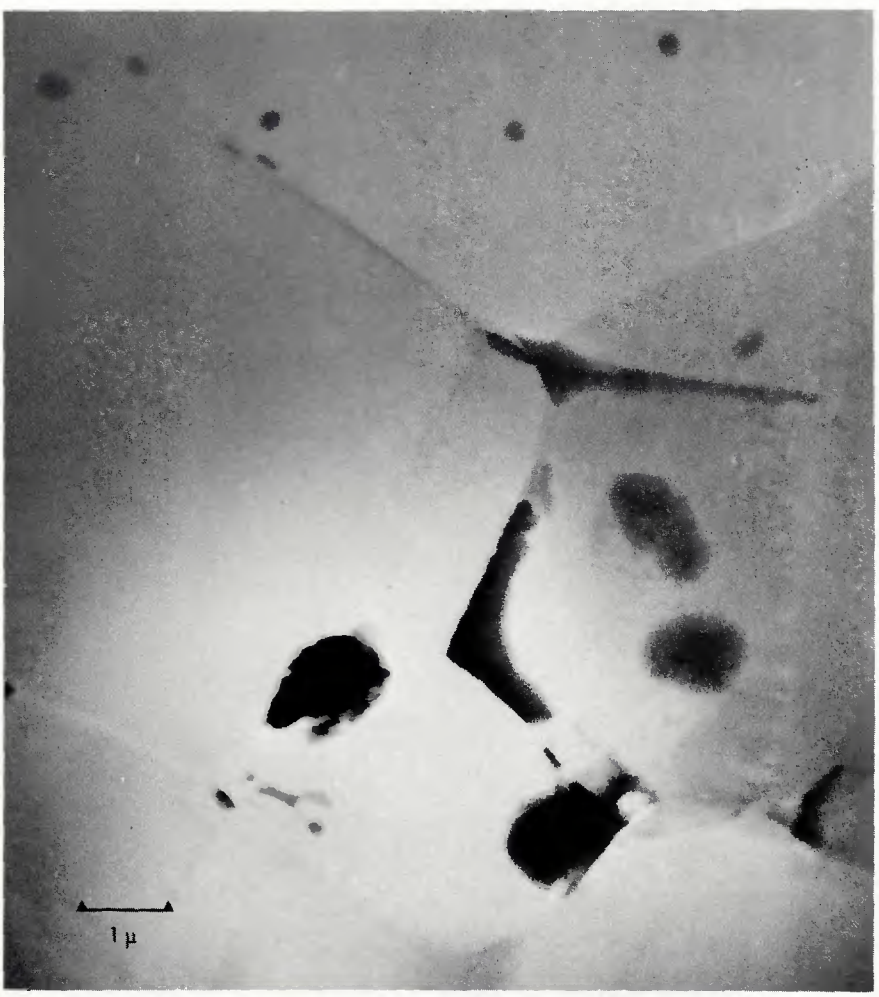

Fig. 12 — Extensive aluminum-rich precipitation along grain bounderies in the vicinity of intergranular cracks in the heat-affected zone

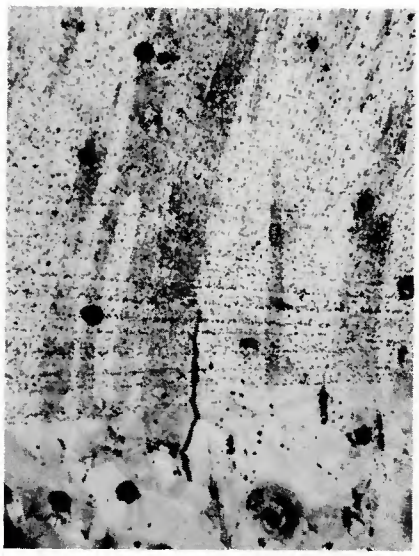

Fig. 13 — Solidification bands across the columnar grains near the edge of the fusion zone. Note the absence of banding in the heat-affected zone at right. (Bright field, X150, reduced 32%)

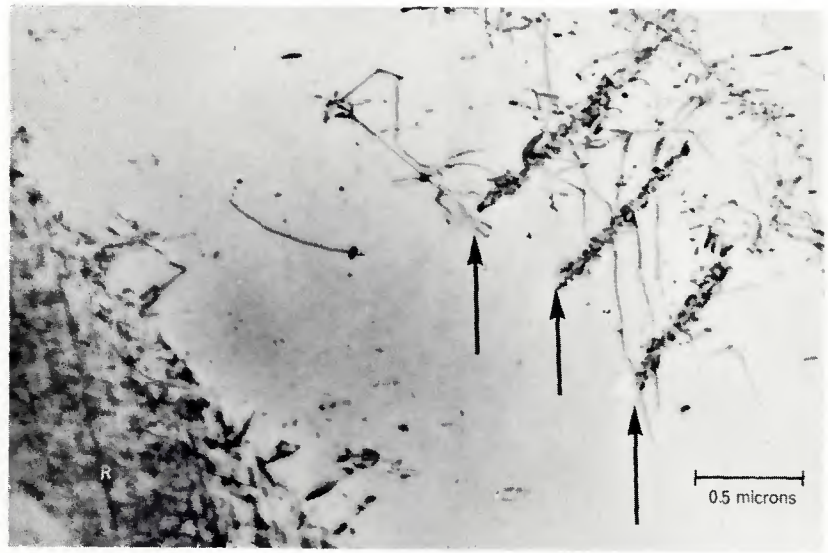

Fig. 14 — Row of platelet shaped precipitates (arrows) inter-connected by dislocation tangles. Another parallel row is noted in region R

solute bands in Be ingot sheet.

The photomicrographs of the fusion zone revealed that these *solidification bands* consisted of rows of both irregular-shaped and platelet precipitates interconnected by dislocation sub-boundaries (Figs. 14, 15 and 16). The platelet precipitates shown in Figs. 14 and 15 reached a length of 2 microns in some instances and were subsequently identified by electron diffraction as the binary compound $FeBe_{11}$. Thus, in areas where there was insufficient aluminum to form the ternary $AlMBe_4$, precipitation continued in the form of the binary, MBe_{11}. Both the rows of precipitates and the interconnecting dislocation tangles preferentially etched during electropolishing to produce the *solute* bands. In the center of the weld, the transverse solute banding was not as pronounced, and Fig. 16 reveals that complex precipitation occurred throughout the microstructure.

Apparently the periodicity in thermal fluctuations[17] which produces the solute-enriched bands varies from the center of the weld to the edge of the fusion zone. Hence, the precipitates do not form distinct rows, but instead are scattered profusely throughout the matrix and columnar grain boundaries. Although the precipitates in the center were generally too small to be individually identified by electron diffraction analysis, the morphology of the precipitates indicates a general mixture of irregular and round $AlFeBe_4$ particles, platelets of $FeBe_{11}$

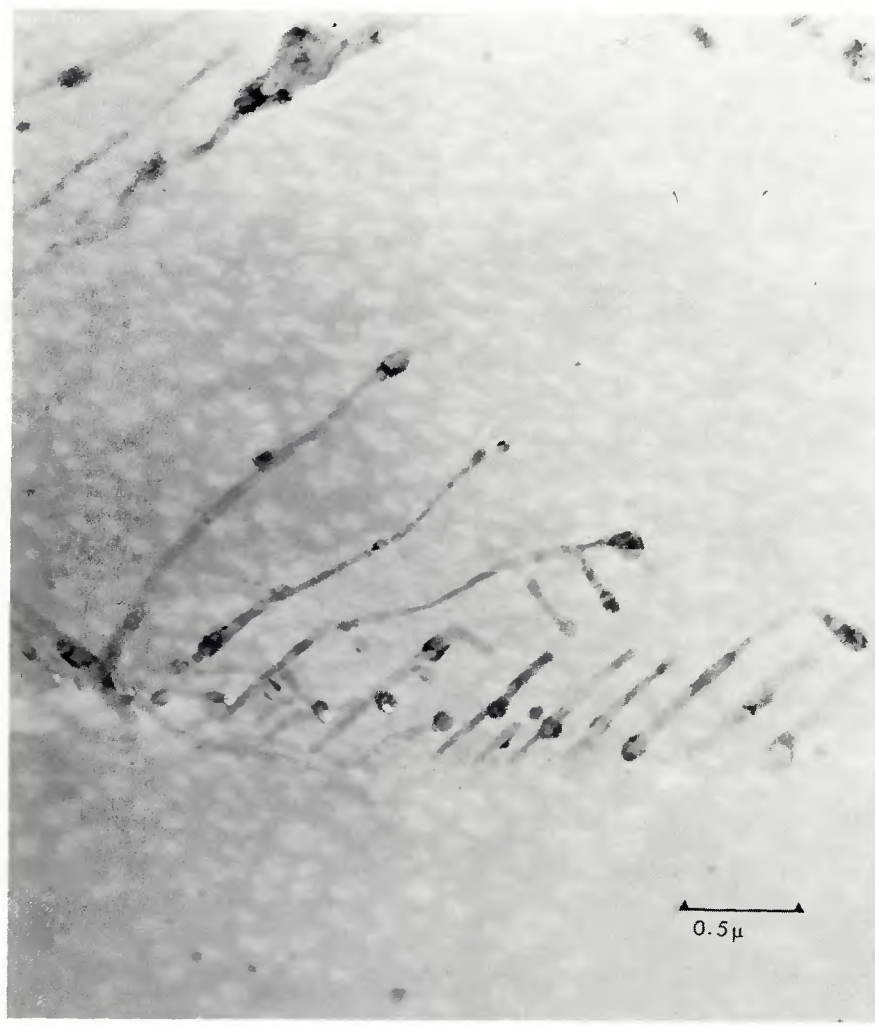

Fig. 15 — Row of precipitates in the fusion zone, identified by electron diffraction patterns as $FeBe_{11}$. Dislocations are tilted out of contrast and are not visible

and occasional long stringers of $AlFeBe_4$. The long stringers of $AlFeBe_4$ were often located in the grain boundaries of the columnar grains, and thus could serve as an additional incentive to intergranular crack propagation in the fusion zone.

Conclusions

The following general conclusions about precipitation in beryllium welds are based on this initial investigation, using beryllium ingot sheet which had been electron beam welded to produce wide heat-affected zones and depth-to-width ratios of about 1 to 1. Hence, caution should be used in extending these results to beryllium which is significantly different in impurity content, since the precipitation characteristics may be significantly altered. Nonetheless, the results are generally applicable to the welding of commercial purity beryllium.

1. The predominant precipitates in the fusion zone and the heat-affected zone were identified by electron diffraction as the ternary type, $AlMBe_4$, and the binary type, MBe_{11}. (In beryllium of Rocky Flats origin, the predominant transition element, M, is Fe so that $AlFeBe_4$ and $FeBe_{11}$ were most often observed in this study.)

2. Transmission electron microscopy revealed extensive aluminum-rich grain-boundary precipitation in the recrystallized heat-affected zone.

3. Electron microprobe scanning revealed a high concentration of aluminum in association with intergranular cracks in the recrystallized zone. It is postulated that the aluminum-rich, grain-boundary precipitates introduce *hot-short* liquid areas which produce the intergranular cracking.

4. Transmission photomicrographs indicate that the *solidification* or *solute* bands in the fusion zone consisted of rows of precipitates interconnected by dislocation tangles and sub-boundaries. However, the precipitation distribution near the center of the fusion zone becomes more random and complex with the result that banding is not as pronounced.

Acknowledgements

The authors express their appreciation to W. G. Booco, H. E. Reed, D. H. Riefenberg, A. W. Brewer, and R. F. Hillyer for their valuable help and discussions.

This work was prepared under Contract AT(29-1)-1106 for the Albuquerque Operations Office, U.S. Atomic Energy Commission.

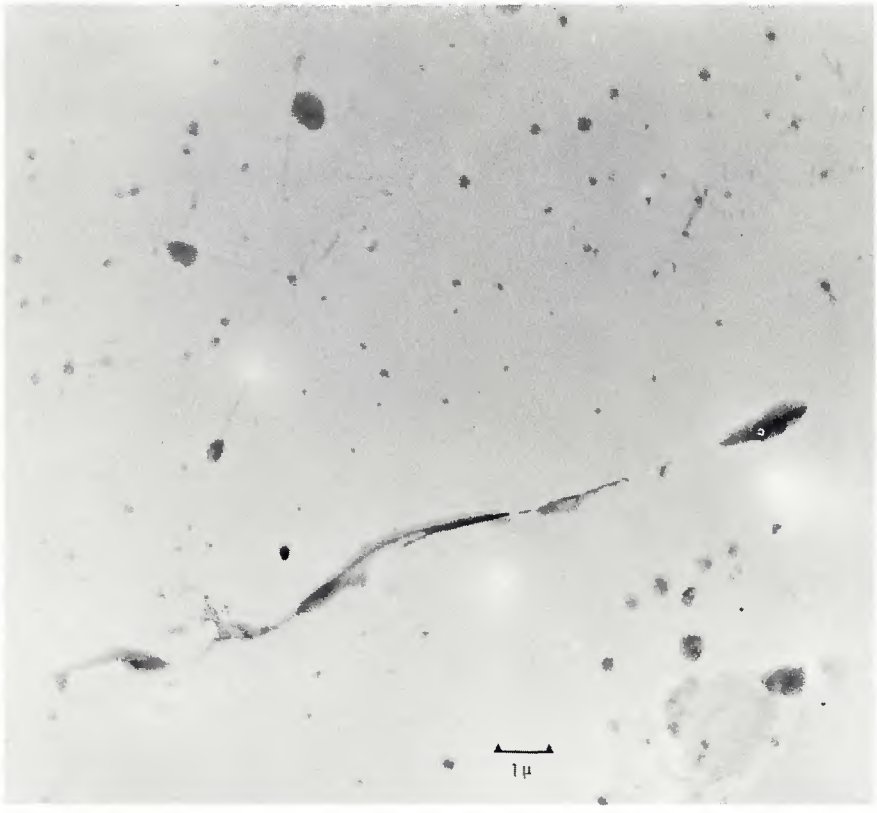

Fig. 16 — Complex precipitation in center of fusion zone of weld. Note long stringer in columnar grain boundary

References

1. Hicken, G. K. and Sample, W. B., Jr., "Joining Beryllium by an Electron Beam Braze Welding Technique," *Welding Journal,* Vol. 46, No. 12, Res. Suppl., pp 541-s to 550-s, 1967.

2. Hicken, G. K., "Effects of Beryllium Oxide on the Braze Weldability of Beryllium," *Welding Journal,* Vol. 47, No. 8, Res. Suppl., pp 364-s to 369-s, 1968.

3. Hauser, D., *et al.,* "Electron Beam Welding of Beryllium," *Welding Journal,* Vol. 46, No. 12, Res. Suppl., pp. 425-s to 540-s, 1967.

4. Hauser, D. and Monroe, R. E., "Electron Beam Welding of Beryllium — Part II," *Welding Journal,* Vol. 47, No. 11, Res. Suppl., pp. 497-s to 514-s, 1968.

5. Jones, A. W. and Weiner, R. T., "The Effect of Heat Treatment on the Mechanical Properties of Some Commercial Beryllium," *Journal of Less Common Metals,* Vol. 6, pp. 266-282, 1964.

6. Moore, A., "Improved Mechanical Properties and Associated Constitutional Changes in Commercially Pure Ingot Beryllium as Affected by Heat Treatment Above 700 C," *Journal of Nuclear Metals,* Vol. 3, p. 113, 1961.

7. Carrabine, J. A., *et al, Beryllium Technology,* Schetky, L. M. and Johnson, H. A., Editors, Vol. 1, pp. 239-257, Gordon and Breach, Science Publishers, New York, 1966.

8. Rooksby, H. P., "Intermetallic Phases in Commercial Beryllium," *Journal of Nuclear Metals,* Vol. 7, pp. 205-211, 1962.

9. Carrabine, J. A., "Ternary $AlMBe_4$ Phases in Commercially Pure Beryllium," *Journal of Nuclear Metals,* Vol. 8, pp. 278-280, 1963.

10. Carrabine, J. A., *et al., Beryllium Technology,* Vol. 1, Scott, V. D. and Lindsay, H. M., pp. 145-178, Gordon and Breach, Science Publishers, New York, 1966.

11. Fraikor, F. J. and Grotzky, V. K., "Grain Boundary Precipitation in Sheet Rolled from Beryllium Ingots," *Transactions of the American Institute of Metallurgical Engineers,* Vol. 239, pp. 2009-2011, 1967.

12. Fraikor, F. J., *et al.,* "Precipitation Characteristics of Rocky Flats Beryllium Ingot Sheet," (RFP-1041), Rocky Flat Division, The Dow Chemical Company, Golden, Colorado. March 12. 1968.

13. Fraikor, F. J., and Brewer, A. W., "Precipitation in Quenched and Aged Beryllium Ingot Sheet," *American Society for Metals Transactions Quarterly,* Vol. 61, pp. 784-789, 1968.

14. Grotzky, V. K. and Fraikor, F. J., "Bright-Field Optical Microscopy of Beryllium," *Journal of Less Common Metals,* Vol. 14, pp. 244-246, 1968.

15. Fraikor, F. J. and Brewer, A. W., "Moire Fringes on Precipitates in Quenched and Aged Beryllium," *Proceedings of the Twenty-Sixth EMSA Meeting,* New Orleans, edited by A. Arceneaux, Claitor's Publishers, pp. 426-427, 1968.

16. D'Annessa, A. T., "Characteristic Redistribution of Solute in Fusion Welding," *Welding Journal,* Vol. 45, No. 12, Res. Suppl., pp. 569-s to 576-s, 1966.

17. Cheever, D. L. and Howden, D. G., "Nature of Weld Surface Ripples," *Welding Journal,* Vol. 48, No. 4, Res. Suppl., pp. 179-s to 180-s, 1969.